

# Analysis of Harmonic Current Propagation in Industrial Sector in Function of the Load Level

João Pedro Trovão<sup>1</sup>, Humberto Jorge<sup>2</sup>

<sup>1</sup> Instituto Superior de Engenharia de Coimbra  
Departamento Engenharia Electrotécnica  
Rua Pedro Nunes, Quinta da Nora – P-3031-199 Coimbra (Portugal)  
phone:+351 239 790 200, fax:+351 239 790 201, e-mail: [jtrovao@mail.isec.pt](mailto:jtrovao@mail.isec.pt)

<sup>2</sup> Dep. de Eng.<sup>a</sup> Electrotécnica e de Computadores  
Faculdade de Ciências e Tecnologia – Universidade de Coimbra  
Pólo II, Pinhal de Marrocos – P-3030-290 Coimbra (Portugal)  
phone:+351 239 796 200, fax:+ 351 239 796 247, e-mail: [hjorge@deec.uc.pt](mailto:hjorge@deec.uc.pt)

**Abstract:** This article presents the influence of the load level variation in the power quality. The study is based on a punctual audit, made to a group of loads in a cement industry, with experimental data acquired by monitoring equipment. Quality indexes of Power Energy Industrial System are determined for different points of the network, such as points of common coupling, disturbing load points, linear load points and reactive energy compensation points. The monitored data are analyzed, according to the patterns of the IEEE 519-1992 standard. Using audit results along with system data, a Power Energy Industrial System simulation model is developed in MATLAB<sup>®</sup>/SIMULINK<sup>®</sup>. This model is then used to extrapolate the Harmonic Distortion Propagation at the industry plant, for other load levels apart from the monitored ones. The information related to Harmonic Distortion Propagation for different load levels is used to strengthen the conclusions of Power Energy Industrial System audits.

**Key words:** Harmonic Distortion Propagation, Power Quality, Industrial plant, Load Level.

## 1. Introduction

In the last years, the static power converters proliferate in the industrial equipments. For example, these devices are frequently used in the speed regulation of electromechanical drives, either with DC motors or induction motors. The use of these devices in installations of electrical energy conversion contributed considerably to improve the performance and efficiency of such systems. However, it has also contributed to the deterioration of the power quality, namely in the current and voltage waveform of the distribution network [1],[2]. These devices are based on power electronics components and possess non-sinusoidal currents, even when fed with a pure sinusoidal voltage. The absorption of non-sinusoidal currents, by elements of these systems, leads to harmonic current circulation, that, due to network impedance, results in supply voltage deformation. [1],[5],[8]

The punctual audits, in Power Energy Industrial System (PEIS), usually focusing on the quality of the current and voltage waveform, can result in rash conclusions with respect to power quality [3]. These inaccurate conclusions are due to the fact that they are based exclusively in the acquisition of the waveform at a certain instant, hence, possibly neglecting other load levels of the system. At the industrial plant is not possible to regulate the load level without disturbing the normal operation of the system. Since for different days at different hours, different conclusions can be achieved, the need to seek alternative or complementary analysis methods is noticeable.

In this article is described a method to starting from a single data acquisition, complemented with simulation work, extrapolate the analyses of one load level to other levels, without the need of a long follow up to analyzing several load levels.

The paper is organized in six sections. Section 2 presents the basic concepts used in this work. Section 3 describes a mathematical analysis, based on fused experimental and simulation results, used to derive the evolution of the feeding waveforms quality indicators as a function of the load level. The fourth section, presents results relative to an audit based on a punctual analysis. Section 5 presents the conclusions obtained by extrapolation analysis, using a combined method (acquired data and simulation results). Finally, the main conclusions of this study are exposed.

## 2. Basic Concepts

Several concepts used in this study, for acquisition system and simulation model are presented in this section. The quantitative indicators used to examine the waveform quality are, the amplitude values of the trigonometric Fourier series decomposition, i.e., the harmonic values ( $X_k$ ) of the  $k$  order, therefore  $X_1$  the fundamental value (1),

$$\begin{aligned}
X_k &= \sqrt{a_k^2 + b_k^2} \\
a_k &= \frac{2}{T} \int_0^T x(t) \cdot \cos k\omega t \, dt, \\
b_k &= \frac{2}{T} \int_0^T x(t) \cdot \sin k\omega t \, dt
\end{aligned} \tag{1}$$

with  $k = 0, 1, 2, \dots$ ,  $\omega = 2\pi f$  and  $f$  is the system frequency, and Total Harmonic Distortion (THD) calculated by

$$THD_X = \sqrt{\sum_{k=2}^{\infty} \left( \frac{X_k}{X_1} \right)^2}, \tag{2}$$

where for electric signals,  $X$  can be a voltage value ( $V$ ) or a current value ( $I$ ) [1],[4],[5].

### A. Data Acquisition System

For the laboratorial study and acquisition in industrial plant, was used a non-invasive acquisition system composed by a commercial portable oscilloscope, a voltage and a current transducers and a personal computer (PC) for data storage (see Fig. 1) [10]. The oscilloscope has two channels, the first is used for acquire a line to line voltage and the second a line current. The transducers are used as a differential voltage probe, for the voltage measurement, and flexible current probe to measure the current with a proportional voltage signal output. The equipment communicates with the PC through a RS-232 connection.

Monitoring medium voltage systems can be accomplished by two distinct ways: directly in the cables and/or supply links (individualized and isolated), requiring that the used transducers have with isolation voltage above the practiced voltage level, or indirectly by the use of instrument transformers. In this study, it was used the indirect method. As stated in [8] the signal adulteration derived the use of the instrument transformers is a common source of error, and by that the signal integrity was verified.

### B. Simulation Models

After an analysis of the available programs for PEIS simulation and considering the intended purpose, it was verified that, for a transitory analysis with models that should be dynamic and of easy structural alteration, MATLAB®/SIMULINK® presents great advantages for the



Fig. 1. Photo of the data acquisition system in industrial plant.

desired study [6],[7],[9]. The simulation models were created using the Power System Blockset, which possesses pre-established blocks of power equipments (Fig. 2) [6]. The implementation of those blocks derives from well studied models, where the most important nonlinear loads are:

- Induction Motor (IM): the used model corresponds to the dynamic model of the asynchronous machine, based on the generalized theory of the electric machinery in the referential stationary (Clarke Transformation).
- Transformer (T): it is based on the classic theory of the electric machinery, using phase equivalent circuit.
- Variable Frequency Drive (VFD): this model combines a three phase diode rectifier model with a three phase Pulse Width Modulation (PWM) inverter model, through a DC link. The control strategy of the inverter corresponds to the technique denominated by vectorial control.

## 3. Variable Frequency Drive Systems

The purpose of this work is the study of Harmonic Distortion Propagation (HDP) evolution as a function of the load level in an industrial plant. As most of the harmonic sources, in cement industries are VFD, an analysis a typical VFD working isolated, was performed. An analysis based on laboratory test and computational simulation, was executed, using a system composed by an IM (400 V; 50 Hz; 12.8 A; 5.5 kW) *EFACEC UNIVERSAL MOTORS S.A.* construction, fed by a commercial VFD (*SIEMENS MICRO MASTER*; 13.5 A; 5.5 kW).

A VFD is typically composed by a three-phase diode rectifier, a DC link and a PWM controlled inverter. This drive differs of the static power converter in some points: it has a diode rectifier that induces a high displacement power factor (DPF), and has a capacitor of great capacity, in the DC link, that regulates the tension. As a result, for light loads (30 to 50%), the current only circulates when the output voltage of the rectifier is above the capacitor voltage. When the load is reduced, the AC side current is discontinuous in a conduction period (see Fig. 3). This operation resembles the “Switch Mode Power Supplies”, except that it is a three-phase circuit high in fifth harmonic current. As the drive load increases, the current tends for continuous, i.e., the conduction time is longer. The point in that the current becomes discontinuous it is determined by the size of the DC link inductance. [2],[8]

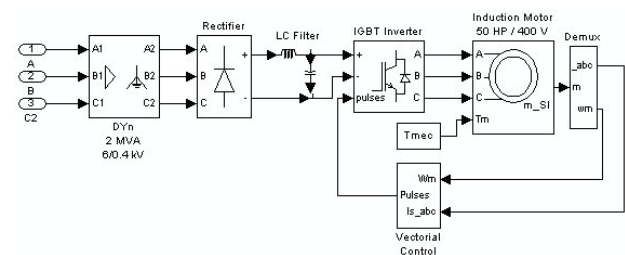


Fig. 2. Block diagram of a MATLAB®/SIMULINK® simulation model.

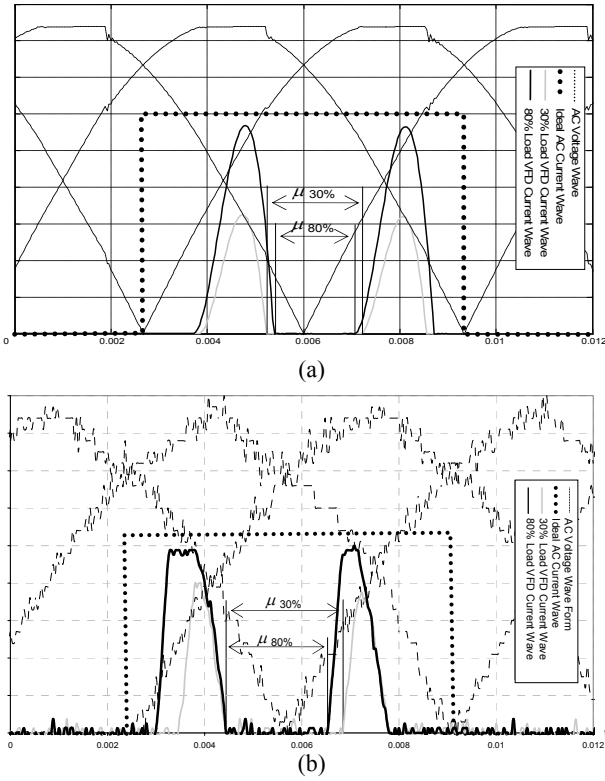


Fig. 3. VFD waveforms. (a). MATLAB<sup>®</sup>/SIMULINK<sup>®</sup> simulation and (b). Laboratory acquisitions.

Considering a DC link without oscillations and perfect commutation, the ideal current waveform absorbed by a rectifier (dotted line in Fig. 3) when feeding a pure inductive load, it is verified that the harmonic component amplitude of the absorbed current are given by

$$I_h = \frac{I_1}{h}, \quad (3)$$

for the case of the six pulses rectifier the harmonic frequencies are,

$$h = 6k \pm 1, \quad (4)$$

where  $k$  is a positive integer, and  $h$  is the harmonic order,  $I_h$  it is the current amplitude of the harmonic order  $h$  and consequently  $I_1$  are the fundamental current amplitude. [5],[8]

As the source that feeds the rectifier is not of infinite power and the semiconductor commutations are not perfect, the expression (3) can be rewritten in function of the commutation angle ( $\mu$ ) [8]:

$$I_h = I_{dc} \cdot \left[ \sqrt{\frac{6}{\pi}} \cdot \frac{\sqrt{A^2 + B^2 - 2AB \cos(\mu)}}{h(1 - \cos \mu)} \right] \cdot \frac{\sin \left[ (h-1) \frac{\mu}{2} \right]}{h-1} \quad (5)$$

$$A = \frac{\sin \left[ (h-1) \frac{\mu}{2} \right]}{h-1}$$

$$B = \frac{\sin \left[ (h+1) \frac{\mu}{2} \right]}{h+1}$$

From Fig. 3 notices that with the load increase the angle  $\mu$  decreases, and (5) demonstrated that with this reduction  $A^1$  and  $B$  also decrease. With load increase, the current in the DC link ( $I_{dc}$ ) proportionally increases, so  $I_h$  increases, but the ratio between the superior harmonics and the fundamental reduces and by that  $THD_i$  also decreases.

The harmonic voltage in a fixed point at the network, is function of the harmonic impedances module at that point ( $Z_{scc}^h$ ) and of the harmonic currents circulation, [4]

$$V_h = \left| Z_{scc}^h \right| \cdot I_h \cdot \quad (6)$$

The network electric impedance at a fixed point is independent of load level. Analyzing (6), if for the  $h$  order,  $Z_{scc}^h$  is constant for any load level, from (5) results that harmonic current amplitude  $I_h$  increases proportionally with the increment of the load level, then the harmonic voltage  $V_h$  also increases with the load level.

For the specific case of the voltage waveform distortion, the expression (2) becomes,

$$THD_v = \sqrt{\sum_{h=2}^{\infty} \left( \frac{V_h}{V_1} \right)^2} \cdot \quad (7)$$

Analyzing (6) and (7), the evolutionary tendency of  $THD_v$  in function of the load corresponds to a gradual increase.

#### 4. Punctual Audit Results

Fig. 4, shows the PEIS in study: a partial industrial installation composed by two power transformers ( $T_1$ ,  $T_2$ ), whose primary one are connected to a same medium voltage link (6 kV) and the secondary feeds several load (linear and non linear). The results of the tests are studied according to the international standard IEEE Std. 519-1992. The installation load is stable during the data acquisition, and by that, the Total Distortion Demand ( $TDD$ ), defined by IEEE for applicability of the 519-1992 Standard, has the same value as the quality index  $THD$  defined in (2) [8].

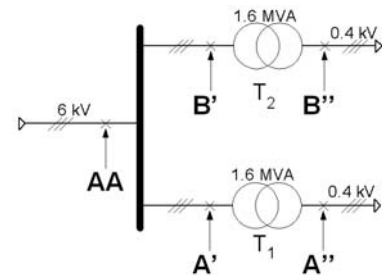


Fig. 4. Scheme of the monitoring PEIS.

<sup>1</sup> For  $h=1$  obtains  $A=1$

### A. Sub-Path A

Fig. 5 shows the voltage and current waveforms in the primary of the transformer  $T_1$  (1.6 MVA; 6/0.4 kV) at the monitoring point A'.

The  $THD_v$  value at this point is below the maximum value allowed by the standard, and by that a significant decrease (4.4%) of the voltage harmonic distortion, in the  $T_1$  primary in relation to the value measured in the secondary (TABLE I), is verified. For the current, it is registered a larger propagation of the harmonic distortion, as the value of measured  $THD_i$  in the primary is similar to the secondary one. This value is above (double of the allowed) the limit imposed by the standard of IEEE.

TABLE I presents the voltage and current characteristic (nontriple odd) harmonics amplitudes and  $THD$ . The current 5.<sup>th</sup> order harmonic is way above the maximum value presented by the norm IEEE 519; however for the voltage they are located inside values limits.

The absorbed current and voltage waveforms at monitoring point A'', acquired in a distribution cabinet that fed several VFDs, a partial cabinet with some linear loads, several IMs and capacitor banks, are shown in Fig. 6. The  $THD_v$  value, at this point, is above the allowed by the norm IEEE 519 by 1%.

TABLE I also shows the characteristic harmonic for the point A'', where the most problematic case is the fifth order. The voltage amplitude is about 2% higher than the IEEE 519 standard and the current amplitude is a value 2.7 times larger than the allowed limit.

TABLE I. – Harmonic amplitude values of the sub-path A

N.º	Harmonic Current Percentages				IEEE Std. 519-1992 Limitations [8]	
	Point A'		Point A''		I [%]	V [%]
5	18.5	1.4	18.5	5.0	7.0	3.0
7	5.7	0.8	5.7	1.4	7.0	3.0
11	3.9	0.5	3.9	2.1	3.5	3.0
13	1.3	0.6	1.3	1.0	3.5	3.0
17	1.0	0.5	1.0	1.0	2.5	3.0
19	1.0	0.7	1.0	0.7	2.5	3.0
23	0.5	0.3	0.5	0.7	1.0	3.0
25	0.2	0.3	0.2	0.5	1.0	3.0
<b>THD [%]</b>	<b>20.5</b>	<b>2.6</b>	<b>20.1</b>	<b>7.0</b>	<b>8.0</b>	<b>5.0</b>

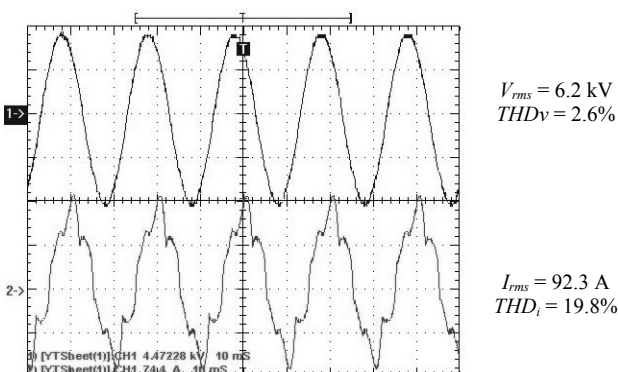


Fig. 5. Voltage and current waveforms at point A'.

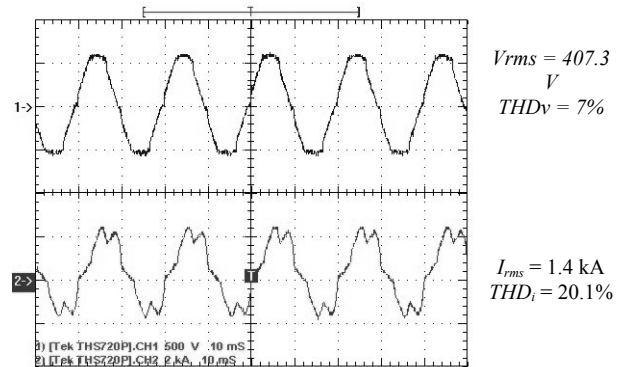


Fig. 6. Voltage and current waveforms at point A''.

### B. Sub-Path B

An analysis similar to the one performed on sub-path A was performed on sub-path B. Fig. 7 and 8 show the voltage and current waveforms at transformer ( $T_2$  - 1.6 MVA; 6/0.4 kV) primary and secondary at the monitoring points B' and B'', respectively. The absorbed current and voltage waveforms at monitoring point B'', are acquired in a distribution cabinet that fed several VFDs, several IMs and capacitor banks. In this data acquisition, the capacitor banks are out of service due to technical reasons.

As it was supposed to happen, the  $THD_i$  value at the point B' is identical to the point A'. The main differences are (TABLE II): the  $THD_v$  at B'' has lowered for half of the value at A'', and is, for this case, below the maximum value allowed by the standard, but still, above the one of

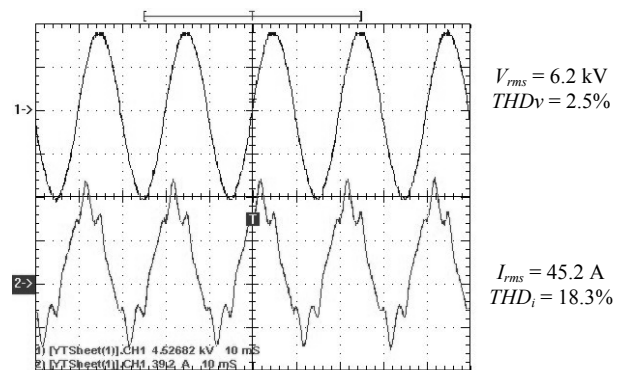


Fig. 7. Voltage and current waveforms at point B'.

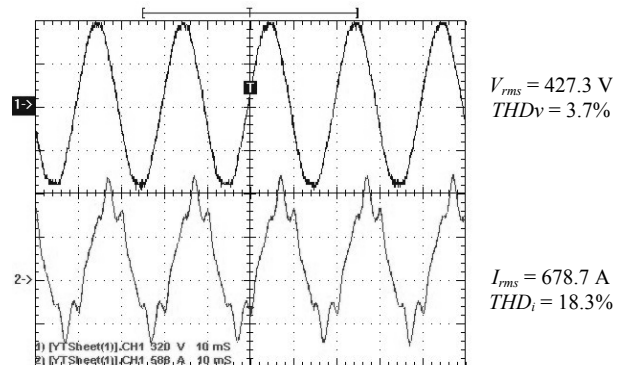


Fig. 8. Voltage and current waveforms at point B''.

B';  $THD_i$  lowered 2% in respect to the value of sub-path A but continued above the limit value; the characteristic voltage harmonics are all inside standard limits; and the seventh order harmonic of the current maintains the same level for both primary and secondary.

TABLE II. – Harmonic amplitude values of the sub-path B

N.º	Harmonic Current Percentages					
	Point B'		Point B''		IEEE Std. 519-1992 Limitations [8]	
	I [%]	V [%]	I [%]	V [%]	I [%]	V [%]
5	12.7	1.4	12.8	1.5	7.0	3.0
7	12.4	0.8	12.2	1.2	7.0	3.0
11	2.5	0.5	2.5	0.4	3.5	3.0
13	0.9	0.4	0.9	0.5	3.5	3.0
17	0.2	0.5	0.2	0.4	2.5	3.0
19	0.4	0.7	0.4	0.1	2.5	3.0
23	0.3	0.3	0.3	0.2	1.0	3.0
25	0.1	0.3	0.1	0.2	1.0	3.0
<b>THD [%]</b>	<b>18.3</b>	<b>2.5</b>	<b>18.3</b>	<b>3.7</b>	<b>8.0</b>	<b>5.0</b>

### C. Point of Common Coupling (PCC) AA

Fig. 9 shows the voltage and current waveforms at the point AA, corresponding to the transformers interconnection medium voltage link (6 kV).

At this point, the  $THD_v$  value is under the maximum value allowed by the IEEE 519 standard, and the  $THD_i$  value is about 4% above the limit proposed by the norm of IEEE.

TABLE III presents that, the characteristic voltage harmonics are located under the limit values, and that the only current harmonic with amplitude above the maximum value of the IEEE 519, is the 250 Hz one.

TABLE III. – Harmonic amplitude values at the point AA

N.º	Harmonic Current Percentages			
	Point AA		IEEE Std. 519-1992 Limitations [8]	
	I [%]	V [%]	I [%]	V [%]
5	14.0	1.4	10.0	3.0
7	5.5	0.8	10.0	3.0
11	4.3	0.5	4.5	3.0
13	1.6	0.6	4.5	3.0
17	1.4	0.5	4.0	3.0
19	0.9	0.7	4.0	3.0
23	0.5	0.3	1.5	3.0
25	0.7	0.3	1.5	3.0
<b>THD [%]</b>	<b>15.9</b>	<b>2.6</b>	<b>12.0</b>	<b>5.0</b>

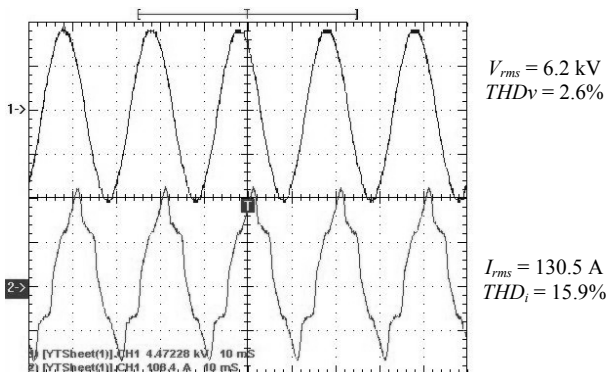


Fig. 9. Voltage and current waveforms at point AA.

The HDP  $THD$  relation, for a specify load level ( $T_1 \rightarrow 61.4\%$ ,  $T_2 \rightarrow 31.4\%$ ), is evaluated in Fig. 10. It is verified that, the current propagation presents almost the same levels for both transformers primary and secondary, nevertheless a decrease of the  $THD_i$  value at the PCC AA is visible. This reduction corresponds to a harmonic attenuation phenomenon of same order, resulting from the addition of deriving currents in that point. For the voltage waveform, at the 6 kV level, a similar value ( $THD_v$ ) is registered for the transformers primary and PCC. However, the low voltage  $THD_v$  levels are higher than the monitored for medium voltage. A special attention should be taken to  $THD_v$  at the point A'' that doubles the value at B''. This results from the significant difference on the current levels that circulates in each branch, and due to the compensation batteries presence in parallel with the loads at A''. This last can create a resonance phenomenon, that amplifies voltage amplitude of some harmonic frequencies and consequently a increases  $THD_v$ .

## 5. Analysis with Data Extrapolation for Simulation

For extrapolating of the data obtained in the punctual audit presented in section 4, a model was developed for the PEIS presented in Fig. 4. This model was implemented in MATLAB®/SIMULINK®, with the Power System Blockset, such as exemplified in section 2. B.

### A. Computational Simulation Model

Before the computational model elaboration, an exhaustive survey of the system in analysis (equipments and identification plate) was performed.

This PEIS study corresponds to a part of an industrial electrical network, whose supply is provided by the *Alto São João* substation (EDP Distribution), where the maximum three-phase short circuit power at the delivery point is 750 MVA (60 kV). The 6 kV points, in the plant internal network, present, for computing and dimensioning, 25 kA of circuit-breaker capacity.

At the PCC point, the short circuit impedance is modelled with the previous values, and type and length of cables. The power transformers ( $T_1$ ,  $T_2$ ), were modelled by the phase equivalent circuit in order to obtain the

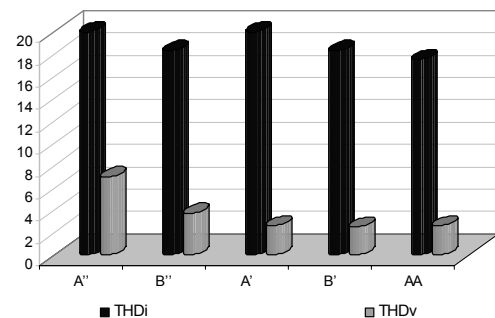


Fig. 10.  $THD_i$  and  $THD_v$  evolution at the monitoring points.

appropriate connections of the windings (Dyn5, 1.6 MVA power, 6/0.4 kV transformation ratio and 6% short circuit voltage).

The connection of the loads to the  $T_1$  and  $T_2$  secondary was modelled by impedances placed in series with the loads, simulating this way the cables and connections.

The loads placed at down of each power transformer, are essentially VFDs (fans), IMs (rug transporters and bombs), linear loads and capacitor banks. TABLE IV presents, for each transformer, a summary of the power by load type. The PEIS characteristics present that, the only equipments with possibility of load variation are the fans supplied by the VFDs.

TABLE IV. – Description of loads supplied by  $T_1$  and  $T_2$

Transf.	VFD Drive		Induction Motor		PF Comp.	Linear Load
	Quant.	Power (kW)	Quant.	Power (kW)	Power (kVA)	Power (kVA)
T1	6	75	1	40	200	140
	2	132				
	2	160				
<b>Total</b>		1034		40	200	140
T2	12	37	1	70	--	250
<b>Total</b>		444		70	--	250

The load level variation, in the VFD drives was implemented in the model by a varying constant that modelled the load torque applied to the IMs of the

electromechanical drives, denominated by  $T_{mec}$  in the generic block diagram presented in Fig. 2.

The electrical machines parameters used in this simulation model were obtained through manufacturers' reference parameters and established pondered values for each power range.

### B. Results and Discussion

Fig. 11 shows the waveforms results, at same points where measured values for audit and with the same load level, of the MATLAB<sup>®</sup>/SIMULINK<sup>®</sup> simulation. These waveforms can be confronted with audit waveform for computational model validation.

These waveforms and the indexes used in the waveforms quality quantification, possesses a satisfactory degree of similitude between the simulation results and the monitored data of the PEIS. The principal differences between both results are due to difficulty of obtain a rigorous model of a complex PEIS system, without the exact parameters of each machine, i.e., the phase equivalent circuit parameters of all electrical circuits. However, these approaches present suitable results and that model can be used to simulate the real process in this study.

Simulations are made with several variants. TABLE V presents the different configurations groups of  $T_1$  and  $T_2$  load levels, and  $THD$ , voltage and current values, in the several monitoring points of the system.

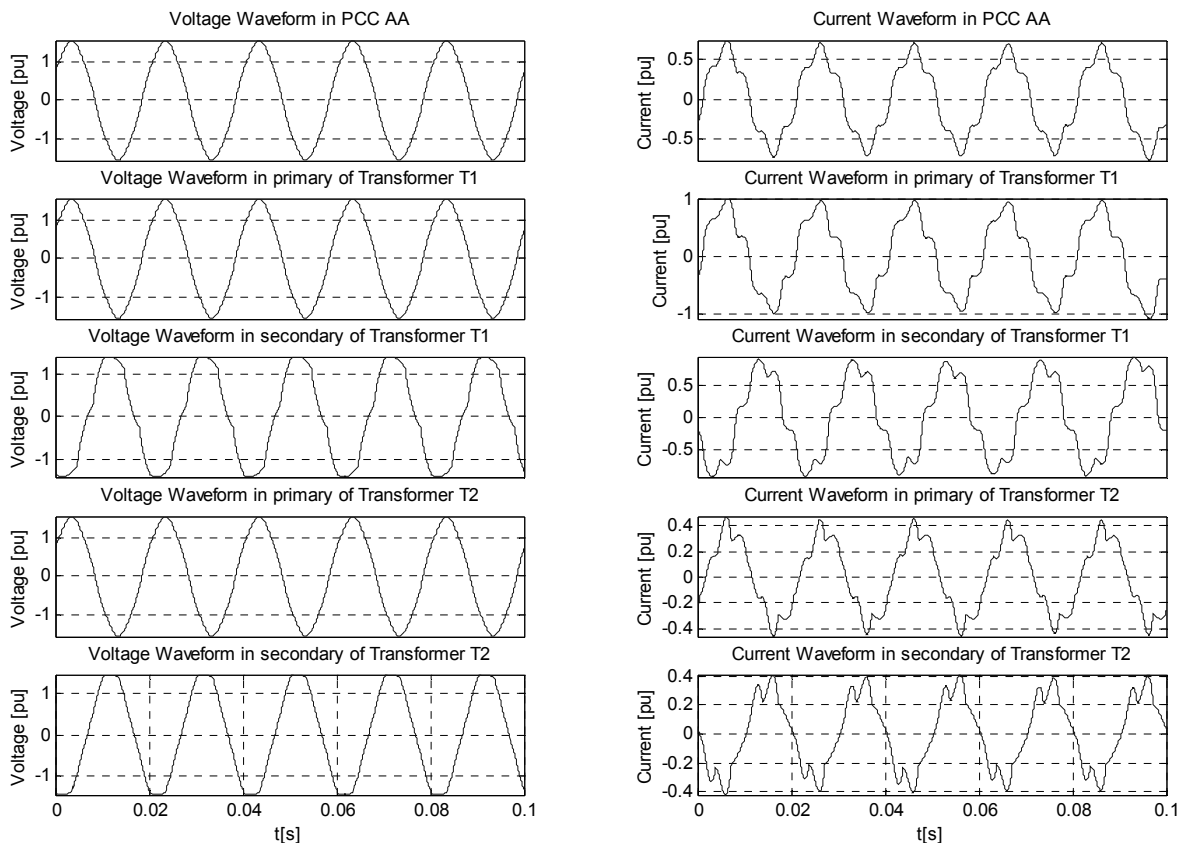


Fig. 11. Simulation results for the load levels monitoring in the audit.

TABLE V. –THD's for different load situations

Situation	S1	S2	S3	S4	S5	S6	S7	S8	S9	
<b>Load Level (%)</b>	<b>T<sub>1</sub></b>	65.0	39.0	38.0	54.0	67.0	66.0	58.0	72.0	38.0
	<b>T<sub>2</sub></b>	28.0	39.0	47.0	35.0	28.0	28.0	48.0	72.0	28.0
<b>Point A''</b>	<b>THD<sub>v</sub> (%)</b>	7.4	5.5	5.7	6.8	7.7	7.5	7.4	9.5	4.9
	<b>THD<sub>i</sub> (%)</b>	19.2	20.4	20.2	20.3	19.5	19.8	19.8	18.3	20.9
<b>Point B''</b>	<b>THD<sub>v</sub> (%)</b>	4.1	5.8	6.7	5.4	4.2	4.2	6.9	10.2	3.9
	<b>THD<sub>i</sub> (%)</b>	19.9	19.3	19.0	19.6	20.0	20.1	18.5	18.0	19.9
<b>Point A'</b>	<b>THD<sub>v</sub> (%)</b>	2.4	2.5	2.7	2.5	2.5	2.4	3.0	4.2	1.9
	<b>THD<sub>i</sub> (%)</b>	20.0	19.3	18.7	19.5	18.8	19.1	19.0	17.6	19.8
<b>Point B'</b>	<b>THD<sub>v</sub> (%)</b>	2.4	2.5	2.7	2.5	2.5	2.4	3.0	4.2	1.9
	<b>THD<sub>i</sub> (%)</b>	17.9	17.2	17.0	17.7	17.9	17.9	16.8	16.5	17.8
<b>Point AA</b>	<b>THD<sub>v</sub> (%)</b>	2.4	2.5	2.7	2.5	2.5	2.4	3.0	4.2	1.9
	<b>THD<sub>i</sub> (%)</b>	17.0	19.4	19.6	18.1	16.5	16.8	18.3	17.5	18.4

The results presented allow two types of study: one about the  $THD$ 's evolution, separately for each monitoring point, in function of the load level increase and another about the  $THD$ 's evolution, at each monitoring points, in function of the several situations proposed.

For the first approach, comes out from Fig. 12 and 13, that for the sub-path A and the sub-path B a load increase, from 25% to 75% of the rate load, in each transformers corresponds to global decrease of about 2% in the  $THD_i$ , in the registered points A', A'', B', and B''.  $THD_v$ , in opposition, increases for both transformers secondary and primary, however the increase for secondary (6%) is greater than for the primary (2%). The discrepancy in the increase rate of  $THD_v$ , between the medium and the low voltage links, depends on the harmonic impedance values at those two points of the industrial electrical network [9].

The limits proposed by the IEEE 519 standard for this type of installation, in terms of harmonic current, are largely surpassed. Even with the decrease presented due to the load increase,  $THD_i$  remains out of the limits. In the best situation doubles the maximum advised value. For the voltage waveform distortion, two different situations are presented, depending if transformers primary or secondary are considered. For primary this value, in spite of increasing with load level, is inside standard imposed limits for all load levels. For the secondary if the load level doesn't overcome 35% of the rate load the  $THD_v$  remains inside of norm limits.

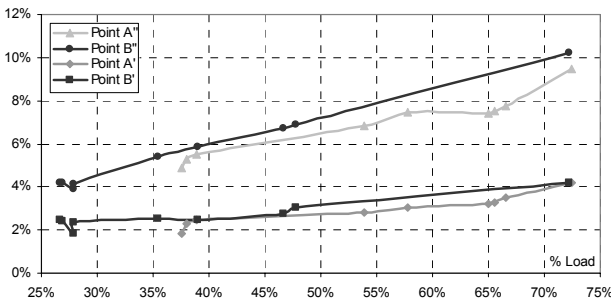


Fig. 12.  $THD_v$  load level function.

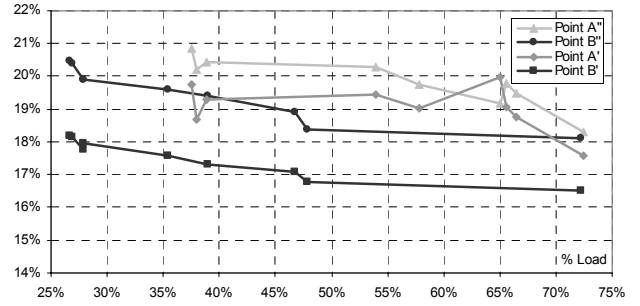


Fig. 13.  $THD_i$  load level function.

The second approach comes out from the possibility of the sub-paths work separately, i.e., the load increase for  $T_1$  may not to be followed by a load increase in  $T_2$ . TABLE V presents values for this type of regime, in situation S1 to S8 are presented different load levels of  $T_1$  and  $T_2$  without any relation between them. However this analysis is justified more at PCC AA, where the different load levels for the two sub-paths, results in a  $THD_i$  evolution that depends on harmonic current level in both sub-paths as well as angular phase.

The voltage waveform distortion is not influenced by different load levels alterations of the  $T_1$  and  $T_2$  transformers. However it depends of the resulting vectorial sum of the harmonic currents absorbed by  $T_1$  and  $T_2$ , and consequently of the load level at point AA.

At the point AA (Fig. 14), the voltage and current waveforms quality indicators, vary in function of the load, in a linear form. The linearization of the  $THD_i$  load level ( $LL_{ch}$ ) relation, results in,

$$THD_i = -0.0472 \cdot LL_{ch} + 0.2085, \quad (8)$$

and for the  $THD_v$  - load level relation

$$THD_v = 0.0559 \cdot LL_{ch} + 0.0014. \quad (9)$$

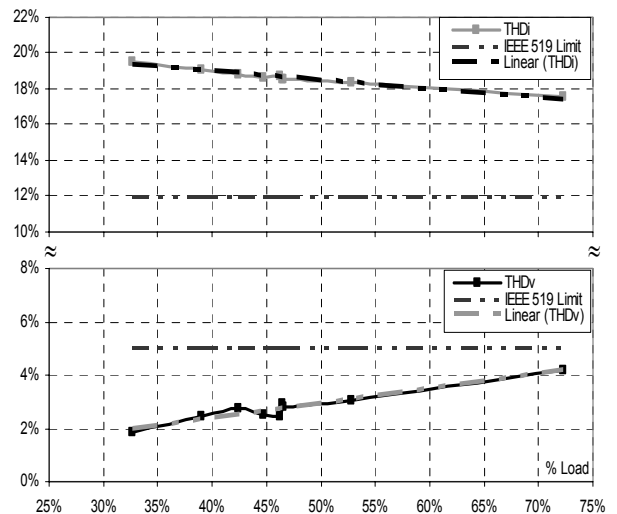


Fig. 14.  $THD_v$  and  $THD_i$  load level function at PCC AA.

The quality index current waveform (8), the rate depends essentially on the non linear loads characteristics with a special focus on the commutation angle  $\mu$  according to the exposed in section 3. Another important factor to this rate is the response of the network to the load variations. For the voltage waveform quality (9), the parameters that influence the  $THD_v - LL_{ch}$  relation are the harmonic current circulation, and system impedance at the different network points due to the different response at distinct frequencies.

In summary, the  $THD_v$  varies directly with load level, with a higher rate in the transformers secondary. The overcome of standard limits for load levels above 35% can compromise the installation of new loads without the implementation of measures that seek the minimization of the 5.<sup>th</sup> e 7.<sup>th</sup> order current harmonics. For the medium voltage link, the voltage harmonic distortion is inside of the IEEE norm limits; however the  $THD_i$  levels are always above the limits. Network expansions must consider these factors.

## 6. Conclusion

In this article is pursued an alternative or complementary analyses method of HDP in a PEIS, that can strengthen conclusions retired from a punctual audit. In this study, the use of simulation system reported is recommended as a possible aid in analysis of HDP. This article explores this possibility, using as starting point a simple punctual audit. A specific model was developed for PEIS, having obtained results about the harmonic distortion evolution in function of the load level. The results allow a reinforcement and improvement of the punctual analysis based on the simple specific time monitoring. This analysis can provide some help in the dimensioning of the harmonic distortion solutions and in the localization of best the insertion point of new loads.

## Acknowledgement

The authors gratefully thanks the CIMPOR Indústria de Cimentos, S.A. - C. P. Souselas, particularly the Mr. José de Sousa Costa, for providing to the opportunity of on site data acquisition.

## References

- [1] DUGAN, R., MCGRANAGHAN, M., WAYNE, H., 1999, *Electrical Power Systems Quality*, 265 pp., McGraw-Hill, NewYork, USA.
- [2] BOSE, K.; *Power Electronics and Variable Frequency Drives, Technology and Applications*; New York: USA, IEEE Press cop., 1997;
- [3] MORINEC, A., *Benefits of Long-Term Power Quality and Power Consumption Monitoring at the Service Entrance Point of Industrial Facilities*, Proceedings of the IEEE PES North American Power Symposium, Phoenix, USA, October 1998.
- [4] DAVIS, E., EMANUEL, A., PILEGGI, D., *Harmonic Pollution Metering: Theoretical Considerations*, IEEE Transactions on Power Delivery, vol. 15, n.º 1, pp. 19-23, January 2000.
- [5] UIE, *Types of Disturbances and Relevant Standards*, Guide to Quality of Electrical Supply for Industrial Installations, "Power Quality" Working Group WG2.
- [6] CHEE-MUN, O, 1998, *Dynamic Simulation of Electric Machinery using Matlab®/Simulink®*; New Jersey: USA, Prentice-Hall, Inc.
- [7] MASWOOD, A., JUN, Z., *Analysis of Harmonic Current Propagation Generated by Power Electronic Controls under Nonideal Conditions*, pp. 551-564, Electric Machines and Power Systems, Volume 28, Number 6, June 2000, Taylor & Francis.
- [8] IEEE STD 519-1992, *IEEE Recommended Practices and Requirements for Harmonic Control in Electric Power Systems*, IEEE Industry Applications Society/Power Engineering Society.
- [9] IEEE PES HARMONIC WORKING GROUP., *Characteristics and Modelling of Harmonic Sources-Power Electronic Devices* , IEEE Transactions on Power Delivery, vol. 16, n.º4, pp. 791-800, October 2001.
- [10] PRETORIUS, J., WYK, J., Swart, P., *An Evaluation of Some Alternative Methods of Power Resolution in a Large Industrial Plant*, IEEE Transactions on Power Delivery, vol. 15, n.º 3, pp. 1052-1059, July 2000.